Chalcogenide Letters Vol. 8, No. 8, August 2011, p. 469-475

STRUCTURAL AND OPTICAL CHARACTERIZATION OF $(Bi_{0.95}Sb_{0.05})_2S_3$ THIN FILMS

P. USHA RAJALAKSHMI[a], RACHEL OOMMEN[a*], C. SANJEEVIRAJA[b], N. JESSY MATHEW[a]

[a]*Department of Physics, Avinashilingam Deemed University for Women, Coimbatore - 641 043, Tamilnadu, India*

[b]*Department of Physics, Alagappa University, Karaikudi- 630 003, Tamilnadu, India*

Polycrystalline $(Bi_{0.95}Sb_{0.05})_2S_3$ thin films are deposited on glass substrates by thermal evaporation technique. The as-deposited and annealed films are characterized by X-ray diffraction, EDAX, atomic force microscopy and UV-Vis. spectrophotometry. Polycrystalline nature of the annealed $(Bi_{0.95}Sb_{0.05})_2S_3$ films is confirmed by X-ray diffraction. The elemental composition of $(Bi_{0.95}Sb_{0.05})_2S_3$ powder and film is estimated from EDAX analysis. Surface morphology of the as-deposited films and the effect of annealing on the morphology of films are examined using atomic force microscopy. Calculated direct optical band gap of the films is in the range of 2.4-2.21 eV and 2-1.55 eV for as-deposited and annealed films respectively.

(Received May 9, 2011; July 28, 2011)

Keywords: Thin films, Thermal evaporation, Bi_2S_3, Sb_2S_3, Solid solution, Optical band gap

1. Introduction

Ternary V-VI compounds of type A_2B_3 (A= Bi and Sb, B= S, Se and Te) are important semiconductor materials due to their low cost and abundance of the constituent elements [1]. The bismuth sulphide (Bi_2S_3) thin film is suitable for photoelectrochemical conversion of solar energy due to its optimum band gap of 1.7 eV [2]. The properties of bismuth sulphide can be tailored by preparing solid solutions with suitable materials. Antimony sulphide (Sb_2S_3) has similar crystallographic properties as that of Bi_2S_3 thereby suggesting possibility of existence of $(Bi_xSb_{1-x})_2S_3$ solid solution. Properties of a number of ternary compound semiconductor thin films [3-12] are reported by various research groups. In the present work an attempt has been made to prepare $(Bi_{0.95}Sb_{0.05})_2S_3$ thin films by thermal evaporation technique. Crystal structure, composition, morphology and optical properties of thermally evaporated $(Bi_{0.95}Sb_{0.05})_2S_3$ solid solution thin films are reported in this paper.

2. Experimental

$(Bi_{0.95}Sb_{0.05})_2S_3$ solid solution thin films are deposited onto microscope slides by thermal evaporation of $(Bi_{0.95}Sb_{0.05})_2S_3$ powder. $(Bi_{0.95}Sb_{0.05})_2S_3$ powder is prepared by solid state reaction route. High purity Bi_2S_3 (Sigma) and Sb_2S_3 (Sigma) powders are thoroughly milled and mixed with mortar and pestle and the pelletized mixture is sintered at 300°C for 3 hours. The crystalline phase formation of the sintered pellet is confirmed by X-ray diffraction. Sintered $(Bi_{0.95}Sb_{0.05})_2S_3$ powder is transferred to a molybdenum boat and thermally evaporated in a Hind Hivac vacuum coating unit (Model:12A4D). Prior to deposition the chamber is evacuated to a base pressure of 10^-

*Corresponding author : rachel12in@yahoo.co.in

^{5} mbar. The source - substrate distance is kept constant at 11 cm. To ensure uniform deposition, the substrate holder is rotated at a constant speed of 12 rpm. During deposition, thickness of the films is monitored using a digital thickness meter. The as-deposited films are annealed at 300° C for two hours. The XRD pattern of the sintered powder, as-deposited and annealed films are recorded using D8 Advance diffractometer operating with Cu K_{α} radiation. The elemental composition of the $(Bi_{0.95}Sb_{0.05})_2S_3$ powder and film are analysed using Energy Dispersive X-ray Spectrometer (INCA Oxford). The surface morphology of the films are scanned using Scanning Probe Microscope (Nanoscope-E) from digital instruments. UV-Vis-NIR spectrophotometer (JASCO V-570) is used to record the optical transmittance spectra of the films.

3. Results and discussion

3.1 Structural Characterization

X-ray diffraction pattern of the Bi_2S_3 thin film, $(Bi_{0.95}Sb_{0.05})_2S_3$ powder, as-deposited and annealed $(Bi_{0.95}Sb_{0.05})_2S_3$ films are shown in figure 1. Broad diffraction peaks observed in the case of Bi_2S_3 thin film (annealed at 200°C) indicates that the deposits consist of fine grains. XRD pattern of the $(Bi_{0.95}Sb_{0.05})_2S_3$ powder exhibits relevant peaks which are indexed to orthorhombic crystal structure of bismuth sulphide. Crystallization is partial in the case of as-deposited $(Bi_{0.95}Sb_{0.05})_2S_3$ film which is evidenced by the XRD pattern. Annealed $(Bi_{0.95}Sb_{0.05})_2S_3$ film is polycrystalline in nature and the grains have a preferred orientation along (020) direction. Comparison of the peak positions in all the diffractograms with the standard data (JCPDS 84-0279) confirms the phase formation of the material in orthorhombic bismuthinite crystal structure. The calculated value of the lattice parameters are a = 3.9827Å, b =11.262 Å, c =11.345 Å.

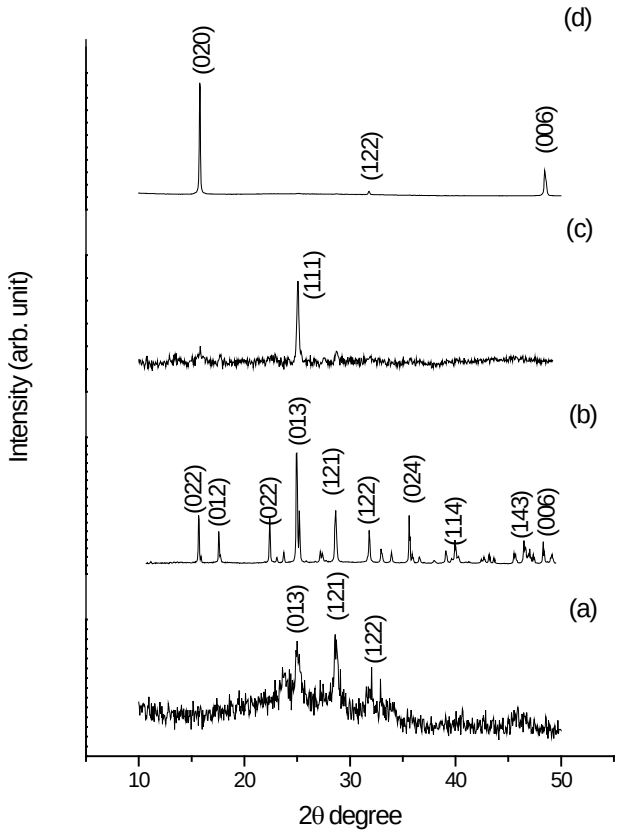

Fig. 1. XRD pattern of (a) Bi_2S_3 thin film (b) $(Bi_{0.95}Sb_{0.05})_2S_3$ powder (c) as-deposited $(Bi_{0.95}Sb_{0.05})_2S_3$ thin film (d) annealed $(Bi_{0.95}Sb_{0.05})_2S_3$ thin film

Empirical relationship describing the relationship between the lattice parameter of a three dimensional solid solution and its composition is known as Vegard's law. The simplest mathematical expression of Vegard's law is [13],

$$a\ (mixture) = (1-x)a_1 + xa_2 \quad (1)$$

where a is the lattice parameter of the mixture, a_1 and a_2 are the lattice parameters of the constituents and x is the molar fraction of the second component. The calculated lattice parameters of the solid solution thin films are related to that of the components through Vegard's law and they are found to obey the law very well. Microstuctural parameters such as grain size, dislocation density and microstrain are calculated from XRD data. Average grain size is calculated using Scherrer formula [14] ,

$$D = 0.9\lambda/\beta \cos\theta \quad (2)$$

where λ is the wavelength of the X-rays used, β is the peak width at half maximum intensity in radian, θ is the Bragg angle of the diffraction peak. Microstrain is calculated from β values using the relation [15]

$$\varepsilon = \beta \cot\theta / 4 \quad (3)$$

Dislocation density is calculated using the relation [16]

$$\delta = n / D^2 \quad (4)$$

where n is the factor which is equal to unity for minimum dislocation density. The calculated values of microstructural parameters are given in table-1.The EDAX spectrum of $(Bi_{0.95}Sb_{0.05})_2S_3$ powder and film are shown in figure.2. It is recognised from the EDAX analysis that the atomic percentage of antimony in $(Bi_{0.95}Sb_{0.05})_2S_3$ powder is lower than the expected value (2%).

Table 1. Microstructural Parameters of annealed Bi_2S_3 and $(Bi_2S_3)_{0.95}(Sb_2S_3)_{0.05}$ films

Sample	Thickness,d (nm)	Average grain size, D (nm)	Dislocation density,δ (10^{14} m^{-2})	Microstrain, ε
Bi_2S_3 film	103	23.1	18	0.00570
$(Bi_2S_3)_{0.95}(Sb_2S_3)_{0.05}$ film	110	38	14	0.00402
	319	76	5.8	0.00331

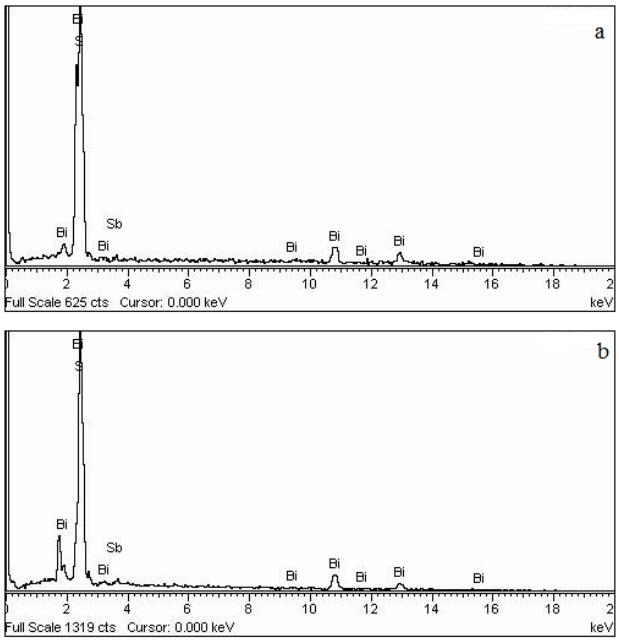

Fig. 2. EDAX spectrum of (a) $(Bi_{0.95}Sb_{0.05})_2S_3$ powder (b) $(Bi_{0.95}Sb_{0.05})_2S_3$ thin film

The atomic percentage of antimony in $(Bi_{0.95}Sb_{0.05})_2S_3$ powder and film is 1.23% and 0.51% respectively. EDAX analysis revealed that the films are non-stoichiometric and contain excessive bismuth. The presence of excessive bismuth in the film may be attributed to the slow rate of evaporation of bismuth (which has pronounced effect at higher evaporation times) when compared to the other constituents in the source material. Figure 3 represents the atomic force micrographs of the as-deposited and annealed $(Bi_{0.95}Sb_{0.05})_2S_3$ films. AFM micrographs reveal that the as-deposited films consisted of uniform grains. Coalescence of the grains is observed in the case of annealed films. Root mean square (RMS) roughness is defined as the standard deviation of the surface height profile from the average height and it is the most commonly reported measurement of surface roughness [17]. RMS roughness of as-deposited and annealed $(Bi_{0.95}Sb_{0.05})_2S_3$ films are calculated using the software "Nanoscope Control 6.13" and the values are presented in table- 2. The RMS roughness of the films is found to increase with annealing.

Table -2 RMS roughness of as-deposited and annealed $(Bi_{0.95}Sb_{0.05})_2S_3$ films

Thickness (nm)	RMS roughness	
	As-deposited	Annealed
54	1.681	2.034
110	1.240	2.208
319	0.938	2.305

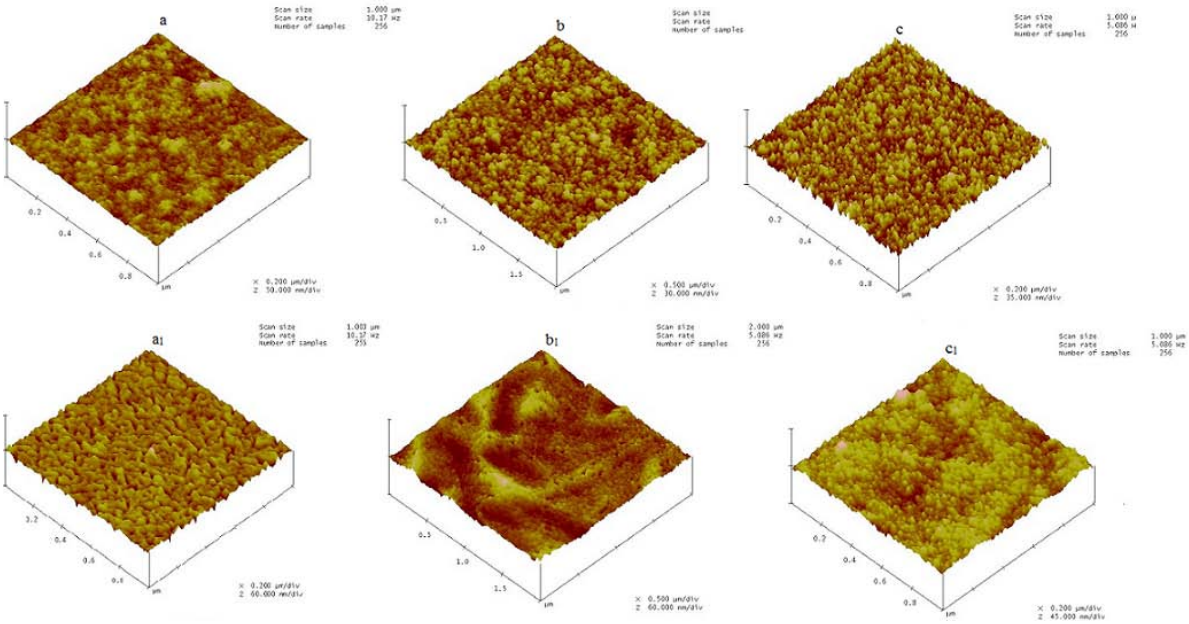

Fig. 3. Atomic force micrographs of as-deposited (a,b,c) and annealed (a_1,b_1,c_1) $(Bi_{0.95}Sb_{0.05})_2S_3$ films of thickness 54 nm, 110 nm, 319 nm

3.2 Optical Characterization

Optical transmittance spectra of the as-deposited and annealed $(Bi_{0.95}Sb_{0.05})_2S_3$ solid solution thin films are shown in figure 4. The films are highly transparent in the NIR region of the electromagnetic spectrum. Annealed $(Bi_{0.95}Sb_{0.05})_2S_3$ films have lower transmittance than the as-deposited films.

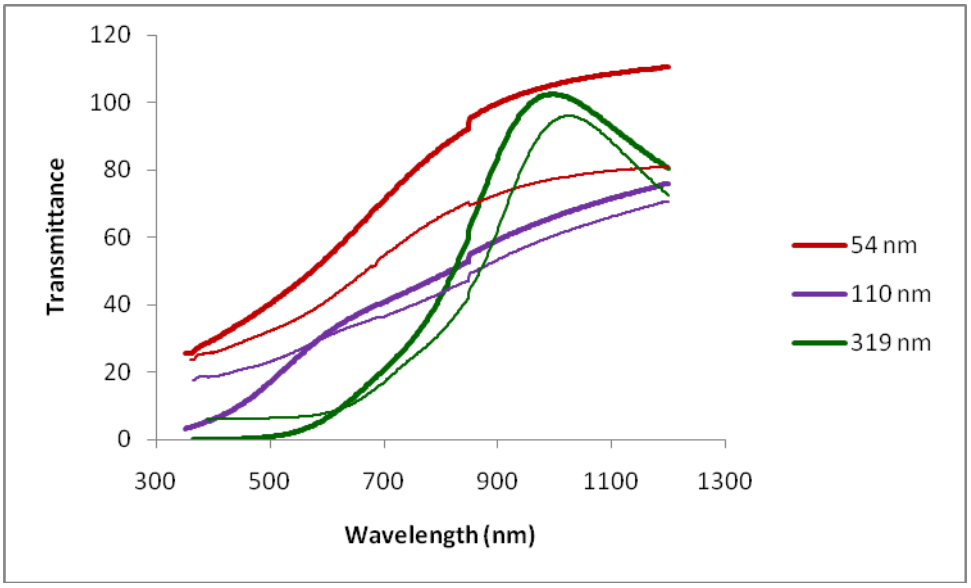

Fig. 4. Transmittance spectra of as-deposited (wide line) and annealed (narrow line) $(Bi_{0.95}Sb_{0.05})_2S_3$ films

The following relationship [18] is used for the determination of absorption coefficient from the transmittance data.

$$\alpha = (1/t)*\ln(1/T) \quad (5)$$

where t, T are film thickness and optical transmittance respectively. The spectral dependence of optical density (αt) of $(Bi_{0.95}Sb_{0.05})_2S_3$ films of varying thickness is shown in figure 5. The films are highly absorbing in the shorter wavelength region.

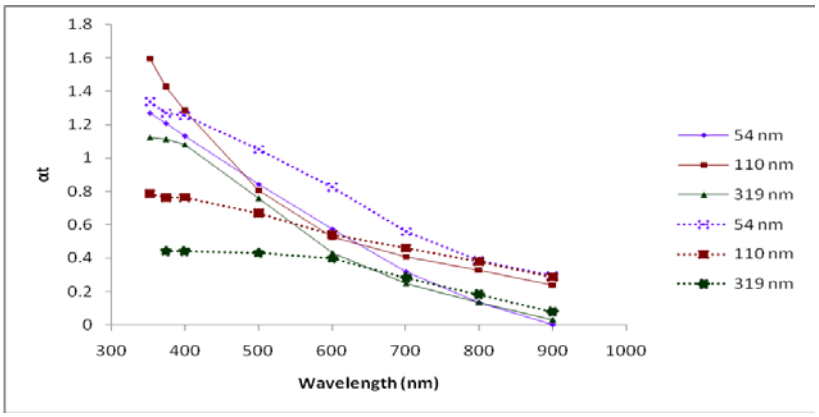

Fig. 5. Variation of optical density of as-deposited (solid line) and annealed (dotted line) $(Bi_{0.95}Sb_{0.05})_2S_3$ films

The nature of the optical transition taking place in the films is determined using Tauc relation [19]

$$\alpha h\nu = A(h\nu - E_g)^n \quad (6)$$

where hν is the photon energy, E_g is the band gap energy, A and n are constants. n = 1/2 for allowed direct transition and n=2 for allowed indirect transition.

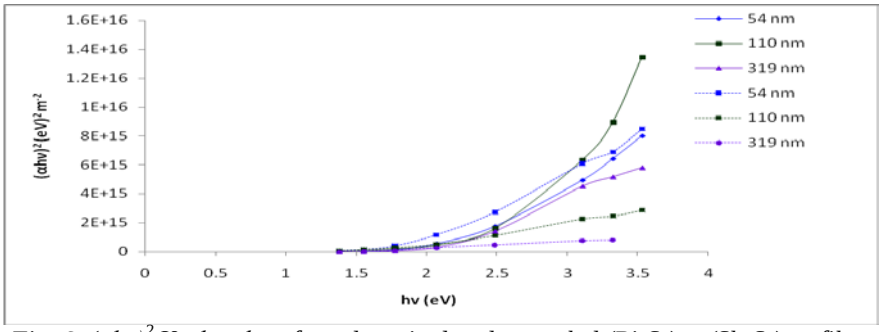

Fig. 6. $(\alpha h\nu)^2$ Vs. hν plot of as-deposited and annealed $(Bi_2S_3)_{0.95}(Sb_2S_3)_{0.05}$ films

Linear nature of the $(\alpha h\nu)^2$ Vs. hν plot (figure 6) indicates that the optical transitions involved are direct and allowed. The value of the band gap is obtained by extrapolating the linear portion of the Tauc plot to the energy axis. Band gap values of as-deposited and annealed films are given in table-3.

Table 3 Optical band gap values of $(Bi_2S_3)_{0.95}(Sb_2S_3)_{0.05}$

Thickness (nm)	Band gap (eV)	
	As-deposited	Annealed
54	2.40	2.0
110	2.35	1.85
319	2.21	1.55

The band gap value decreases with annealing which may be attributed to the improvement of grain size in the annealed films. A red shift in band gap is observed as the thickness of the films

increase. The band gap value of $(Bi_{0.95}Sb_{0.05})_2S_3$ films obtained in the present study is lower than the band gap values of $(Bi_{0.5}Sb_{0.5})_2S_3$ thin films deposited by electrodeposition technique [1].

4. Conclusion

Thin films of $(Bi_{0.5}Sb_{0.5})_2S_3$ are prepared by the thermal evaporation of $(Bi_{0.5}Sb_{0.5})_2S_3$ powder. $(Bi_{0.5}Sb_{0.5})_2S_3$ films annealed at 300°C are polycrystalline and exhibited orthorhombic crystal structure. Lattice parameters of the $(Bi_{0.5}Sb_{0.5})_2S_3$ solid solution films obeyed Vegard's law. The films have high absorption coefficient in the visible region. The direct optical band gap of the as-deposited $(Bi_{0.5}Sb_{0.5})_2S_3$ films is in the range of 2.4-2.21 eV. The band gap of the films decreased with annealing and the band gap values of annealed films range from 2-1.55 eV.

Acknowledgement

The authors gratefully acknowledge Prof. Ajay Gupta, Centre director, UGC-DAE CSR, Indore Centre, for providing characterization (XRD, EDAX, AFM) facilities and Department of Science and Technology, Govt. of India for the financial support.

References

[1] S.Subramanian, Chitra lekha P., Pathinettam Padiyam D., Journal of Non-Crystalline Solids, **356**, 1173 (2010)
[2] L.M.Peter, J. Electroanal. Chem., **98**, 49 (1979)
[3] M.M.Wakkad, J. Phys. Chem. Solids, **51**, 1171(1990)
[4] L.Bu, W.Wang, Appl. Surf. Sci., **253**, 3360 (2007)
[5] E.Benamar, M.Rami, M.Fahouma, F.Chraibi, A.Ennaui, Solid State Sci., **L1**, 301(1999)
[6] B.Subramanian, C.Sanjeeviraja, M.Jeyachandran, Mater. Res. Bull. **38**, 899 (2003)
[7] E.Koukarenk, N.Freti, V.G.Shepelevich, J.C.Tedennac, J. Alloys Compd., **327**, 1 (2001)
[8] M.Takashiri, S.Tanaka, M.Takiishi, M.Kihare, K.Miyazaki, H.Tsukamoto, J. Alloys Compd., **462**, 351 (2008)
[9] A.Mzerd, F.Tcheliebou, A.Sackda, A.Boyer, Sens. Actuators, A **46** , 387 (1995)
[10] D.D.Frari, S.Diliberto, N.Stein, C.Baulanger, J.M.Lecuire, Thin Solid Films, **483**, 44 (2005)
[11] V.A.Patil, A.R.Patil, A.W.Choi, D.S.Palik, S.J.Yoon, Surf. Eng., **23**, 28 (2007)
[12] H.Sasaki, K.Shibayama, M.Tchimura, K.Masui, J.Cryt. growth, **237-239**,2125 (2002)
[13] G.P.Kostikova, Y.P.Kostikov, Inorg. Mater., **29**, 1005 (1993)
[14] B.D.Cullity, Elements of X-ray diffraction, Addison-Wesly, USA , (1956)
[15] D.W.Richards, R.J.De Angelis, M.P.Kramer, J.W.House, D.A.Cunard, D.P.Shea, Adv. X-ray Analysis, **47**, 351 (2004)
[16] Poulomi Roy, Suneel Kumar Srivastava, Thin Solid Films, **496**, 293 (2006)
[17] T.Jiang, N.Hall, A.Ho, S.Morin, Thin Solid Films, **417**, 76 (2005)
[18] S.Subramanian, P.Chitra lekha, D.Pathinettam Padiyam, Current Applied Physics **9**,1140 (2009)
[19] J.Tauc, R.Grigorovici, A.Vancu, Phys. Status Solidi, **15**, 627 (1966)